IOP Conf. Series: Journal of Physics: Conf. Series **1291** (2019) 012007 doi:10.1088/1742-6596/1291/1/012007

The low energy physics of quarkonium suppression in heavy ion collisions

L Abreu, F S Navarra and M Nielsen

Instituto de Física, Universidade de São Paulo, Rua do Matão Travessa R, 187, 05508-090 São Paulo, SP, Brazil

E-mail: navarra@if.usp.br

Abstract.

In the late stage of relativistic heavy ion collisions there is a hadron gas phase, where particles interact at energies of the order of the temperature, i.e., $\simeq 100 - 150$ MeV. We discuss heavy quarkonium production and dissociation in this hot hadron gas. We review the theory giving special emphasis to our recent works on J/ψ and Υ suppression in interactions with pions.

1. Introduction

It is now a well accepted fact that in high energy heavy ion collisions a deconfined medium is created: the quark gluon plasma (QGP) [1, 2]. Indeed, a significant part of the RHIC and LHC physics program is devoted to determine and understand the properties of the QGP. This is the result of a long history.

In 1986, in a famous paper by Matsui and Satz [3] charmonium suppression was proposed as a signal of quark gluon plasma formation. Soon after, bottomonium suppresion was also considered as a tool to study the properties of QGP. At that point, all the accumulated experience with particle production indicated that the multiplicities of all kinds of particles tend to increase with the energy. Therefore the suppression of charmonium was an extremely novel and unfamiliar idea. The physics behind the suppression was simple. In a plasma there is color charge screening and so the would-be quark and anti-quark partners can not "see" themselves and bind together.

In the nineties, charmonium suppression was searched for in heavy ion collisions at the CERN-SPS. Some signs of suppression were found and hence for some authors the credit for the discovery of quark-gluon plasma had to be given to the CERN NA-35 and NA-50 Collaborations.

In 2001, in a very influential paper, Thews, Schroedter and Rafeslki [4] proposed that, in contrast to previous expectations, *charmonium enhancement* was the real signature of QGP. This enhancement would be essentially due to the residual screened Coulomb binding potential and to the large number of charm quarks and antiquarks coexisting in the QGP.

From the experimental side, RHIC started to operate in 2000 and the new data showed no extra suppression with respect to the SPS data, although the cms energy was ten times higher. At this point the community started to believe that both processes were happening. The suppression of the initially formed bound states was stronger and at the same time the recombination was responsible for an enhancement of the $c - \bar{c}$ bound states. Thus the net result was a suppression

very similar to that previously observed but produced by a very different dynamics. In particular there was a prediction that, at even higher energies regeneration would take over and eventually we would see at the LHC an absence of suppression or "unsuppression". Ten years later this expectation would be confirmed by the LHC data.

In parallel to the evolution of the ideas about the dynamics of the quark gluon plasma, some work was also dedicated to understand what happens to all produced particles and also to heavy quarkonium, after the reconfinement phase transition, or hadronization. In a high energy heavy ion collision the QGP is formed, expands, cools, hadronizes and is converted into a hadron gas, which lives up to 10 fm/c and then freezes out. The particles formed during the QGP phase or at its end have to evolve in the middle of a strongly interacting hadronic medium. During this phase heavy quarkonium can be destroyed in the interaction with light mesons and then can be reformed again. For example, in the case of the J/ψ we can have

$$J/\psi + \pi \to D + \bar{D} \tag{1}$$

and also

$$D + \bar{D} \to J/\psi + \pi \tag{2}$$

Similar equations can be written for vector mesons (D^*), for excited charmonium states ($\psi^{'}$) and also for bottom mesons (Υ, B, B^*, ...etc). An interesting aspect of these reactions is that they happen at relatively low energies, tipically of the order of the temperature, i. e., $100 - 150$ MeV. Hence these final state interactions show that high energy collisions contain also low energy subprocesses.

Already in 1998, in a paper by Matinyan and Mueller [5] the theory of the interactions between charmonium and ordinary hadrons was developed to give a precise estimate of how strongly the charmonium is absorbed by a hadronic medium. Hadronic absorption was considered as a background for the most important suppression, which happened in the QGP, as a result of the color screening effect. This theory was based on effective Lagrangians with SU(4) symmetry and since then it has been improved by different authors. A very important improvement was the introduction of "anomalous parity interactions" (or simply anomalous interactions) done by Oh, Song and Lee in 2001 [6]. These interactions were shown to change the cross sections by two orders of magnitude. A subsequent improvement was to extend this kind of theory to the SU(5) symmetry and treat the analogous problem of the interaction between an Υ and a light meson. This was done in 2001 by Lin and Ko [7].

In this contribution we briefly review the theory of hadron interactions applied to heavy quarkonium and discuss the results obtained in our recent publications. In the next sections we present the development of the calculations for charmonium. The calculation steps for the bottomonium are essentially the same and, for the sake of conciseness, we only show the results. In the end we present some concluding remarks.

2. The cross sections

Now we briefly describe the calculation of the cross sections for the $\varphi - J/\psi$ interactions, where φ denotes a pseudoscalar or vector meson. For more details we refer the reader to [8]. The relevant Lagrangians are given by:

$$\begin{aligned}
\mathcal{L}_{PPV} &= -ig_{PPV}\langle V^{\mu}[P, \partial_{\mu}P]\rangle, \\
\mathcal{L}_{VVV} &= ig_{VVV}\langle \partial_{\mu}V_{\nu}\,[V^{\mu}, V^{\nu}]\rangle, \\
\mathcal{L}_{PPVV} &= g_{PPVV}\langle PV^{\mu}[V_{\mu}, P]\rangle, \\
\mathcal{L}_{VVVV} &= g_{VVVV}\langle V^{\mu}V^{\nu}[V_{\mu}, V_{\nu}]\rangle,
\end{aligned} \tag{3}$$

where the indices PPV and VVV, $PPVV$ and $VVVV$ denote the type of vertex incorporating pseudoscalar (P) and vector (V) meson fields in the couplings and g_{PPV}, g_{VVV}, g_{PPVV} and g_{VVVV} are the respective coupling constants. The symbol $\langle \ldots \rangle$ stands for the trace over $SU(4)$-matrices. In the derivation of the SU(4) theory of meson interactions, one works first with mathematical states. The physical states are combinations of the mathematical states. Usually one assumes what is called "ideal mixing", which means that the physical states are just described by their most important components. The matrix V_μ is parametrized by 16 vector-meson fields including the 15-plet and singlet of $SU(4)$. P is a matrix containing the 15-plet of the pseudoscalar meson fields, written in the physical basis in which η, η' mixing is taken into account.

In addition to the terms given above, we also consider anomalous parity terms. The anomalous parity interactions with vector fields can be described in terms of the gauged Wess-Zumino action [6], which can be summarized as

$$\begin{aligned}
\mathcal{L}_{PVV} &= -g_{PVV}\varepsilon^{\mu\nu\alpha\beta}\langle \partial_\mu V_\nu \partial_\alpha V_\beta P\rangle, \\
\mathcal{L}_{PPPV} &= -ig_{PPPV}\varepsilon^{\mu\nu\alpha\beta}\langle V_\mu(\partial_\nu P)(\partial_\alpha P)(\partial_\beta P)\rangle, \\
\mathcal{L}_{PVVV} &= ig_{PVVV}\varepsilon^{\mu\nu\alpha\beta}\left[\langle V_\mu V_\nu V_\alpha \partial_\beta P\rangle \right. \\
&\quad \left. + \frac{1}{3}\langle V_\mu(\partial_\nu V_\alpha)V_\beta P\rangle\right]. \qquad (4)
\end{aligned}$$

The g_{PVV}, g_{PPPV}, g_{PVVV} are the coupling constants of the PVV, $PPPV$ and $PVVV$ vertices, respectively [6]. The couplings given by the effective Lagrangians in Eqs. (3) and (4) allow us to study the following $\varphi J/\psi$ absorption processes

$$\begin{aligned}
&(1)\ \varphi J/\psi \rightarrow D_{(s)}\bar{D}, \\
&(2)\ \varphi J/\psi \rightarrow D^*_{(s)}\bar{D}^*, \\
&(3)\ \varphi J/\psi \rightarrow D^*_{(s)}\bar{D}, \\
&(4)\ \varphi J/\psi \rightarrow D_{(s)}\bar{D}^*, \qquad (5)
\end{aligned}$$

where the final states with strange charmed mesons stand for the initial states with K and K^* mesons, while final states with unflavored charmed mesons appear for the initial states with pions and ρ mesons. The diagrams considered to compute the amplitudes of the processes above are of two types: one-meson exchange and contact graphs. They are shown in Fig. 1 of Ref. [6].

We define the invariant amplitudes for the processes (1)-(4) in Eq. (5) involving $\varphi = \pi, K$ mesons as

$$\begin{aligned}
\mathcal{M}_1^{(\varphi)} &= \sum_i \mathcal{M}_{1i}^{(\varphi)\mu}\epsilon_\mu(p_2), \\
\mathcal{M}_2^{(\varphi)} &= \sum_i \mathcal{M}_{2i}^{(\varphi)\mu\nu\lambda}\epsilon_\mu(p_2)\epsilon^*_\nu(p_3)\epsilon^*_\lambda(p_4), \\
\mathcal{M}_3^{(\varphi)} &= \sum_i \mathcal{M}_{3i}^{(\varphi)\mu\nu}\epsilon_\mu(p_2)\epsilon^*_\nu(p_3), \\
\mathcal{M}_4^{(\varphi)} &= \sum_i \mathcal{M}_{4i}^{(\varphi)\mu\nu}\epsilon_\mu(p_2)\epsilon^*_\nu(p_4). \qquad (6)
\end{aligned}$$

In the above equations, the sum over i represents the sum over all diagrams contributing to the respective amplitude; p_j denotes the momentum of particle j, with particles 1 and 2 standing for initial state mesons, and particles 3 and 4 for final state mesons; $\epsilon_\mu(p_j)$ is the polarization vector related to the respective vector particle j. The explicit expressions of amplitudes $\mathcal{M}^{(\pi)}$ and $\mathcal{M}^{(K)}$ may be found in Ref. [6].

In the case of processes involving $\varphi = \rho, K^*$ mesons, we must add on the right hand side of each expression in Eq. (6) the contraction of the amplitude with the polarization vector of a vector meson, i.e. for the reaction (1) we have $\mathcal{M}_1^{(\varphi)\mu\nu}\epsilon_\mu(p_1)\epsilon_\nu(p_2)$ and so on. The explicit expressions of the amplitudes $\mathcal{M}^{(\rho)}$ and $\mathcal{M}^{(K^*)}$ used here are those published in Refs. [6] and [9, 10].

We are interested in the determination of the isospin-spin-averaged cross section for the processes in Eq. (5), which in the center of mass (CM) frame is defined as

$$\sigma_r^{(\varphi)}(s) = \frac{1}{64\pi^2 s}\frac{|\vec{p}_f|}{|\vec{p}_i|}\int d\Omega \overline{\sum_{S,I}}|\mathcal{M}_r^{(\varphi)}(s,\theta)|^2, \tag{7}$$

where $r = 1, 2, 3, 4$ labels $\varphi - J/\psi$ absorption processes according to Eq. (6); $\sqrt{s}$ is the CM energy; $|\vec{p}_i|$ and $|\vec{p}_f|$ denote the three-momenta of initial and final particles in the CM frame, respectively; the symbol $\overline{\sum_{S,I}}$ represents the sum over the spins and isospins of the particles in the initial and final state, weighted by the isospin and spin degeneracy factors of the two particles forming the initial state for the reaction r, i.e.

$$\overline{\sum_{S,I}}|\mathcal{M}_r|^2 \;=\; \frac{1}{g_1 g_2}\sum_{S,I}|\mathcal{M}_r|^2, \tag{8}$$

with $g_1 = (2I_{1i,r}+1)(2S_{1i,r}+1), g_2 = (2I_{2i,r}+1)(2S_{2i,r}+1)$ being the degeneracy factors of the initial particles 1 and 2.

We employ the isospin-averaged masses: $m_\pi = 138.1$ MeV, $m_\rho = 775.2$ MeV, $m_K = 495.6$ MeV, $m_{K^*} = 893.7$ MeV, $m_D = 1867.2$ MeV, $m_{D^*} = 2008.6$ MeV, $m_{D_s} = 1968.3$ MeV, $m_{D_s^*} = 2112.1$ MeV, $m_{J/\psi} = 3096.9$ MeV. Besides, the values of coupling constants appearing in the expressions of the amplitudes have been taken from Ref. [6] for $\mathcal{M}^{(\pi)}$; from Refs. [9, 10] for $\mathcal{M}^{(K)}$ and $\mathcal{M}^{(K^*)}$; and from Ref. [6] for the couplings involving ρ meson in $\mathcal{M}^{(\rho)}$. We have also included form factors in the vertices when evaluating the cross sections. They were taken from [6] and are:

$$F_3 = \frac{\Lambda^2}{\Lambda^2 + \mathbf{q}^2}; \;\; F_4 = \frac{\Lambda^2}{\Lambda^2 + \bar{\mathbf{q}}^2}\frac{\Lambda^2}{\Lambda^2 + \bar{\mathbf{q}}^2}, \tag{9}$$

where F_3 and F_4 are the form factor for the three-point and four-point vertices, respectively; $\mathbf{q} = (\mathbf{p_1} - \mathbf{p_3})^2$ or $(\mathbf{p_2} - \mathbf{p_3})^2$ for a vertex involving a t- or u-channel meson exchange; and $\bar{\mathbf{q}} = [(\mathbf{p_1} - \mathbf{p_3})^2 + (\mathbf{p_2} - \mathbf{p_3})^2]/2$. The cutoff parameter Λ was chosen to be $\Lambda = 2.0$ GeV for all vertices [6].

As one can see, the Lagrangian theories suffer from two main deficiencies: i) the coupling constants are not known and ii) to regularize the theory and to account for the finite extension of hadrons one is forced to introduce form factors. The functional form of these form factors is unknown. Moreover they contain a cut-off parameter (usually called Λ) which is completely unknown.

The coupling constants can be determined if we use the SU(4) symmetry and some experimental input, such as the $g_{D^*D\pi}$ coupling constant, which is measured in the $D^* \to D\pi$ decay. Other needed coupling constants and also all the form factors can be evaluated with QCD sum rules [11]. Moreover one can compare the results obtained with effective Lagrangian with the cross sections directly computed with QCD sum rules [12]. After five years (1998 - 2003) of combined efforts the community arrived at a consensus on the values of certain cross sections, such as the $J/\psi - \pi$ cross section.

How the existence of a hot hadron gas phase affects the production of J/ψ ? In Eqs. 1 and 2 we show the possible reactions which may change the multiplicity of J/ψ's. They are related by

detailed balance. The matrix element is the same in both directions but the spin-isospin factors are different and also the phase-space is different. For this reason absorption and production do not have the same probabilities. A comparison between both processes is shown in Fig. 1.

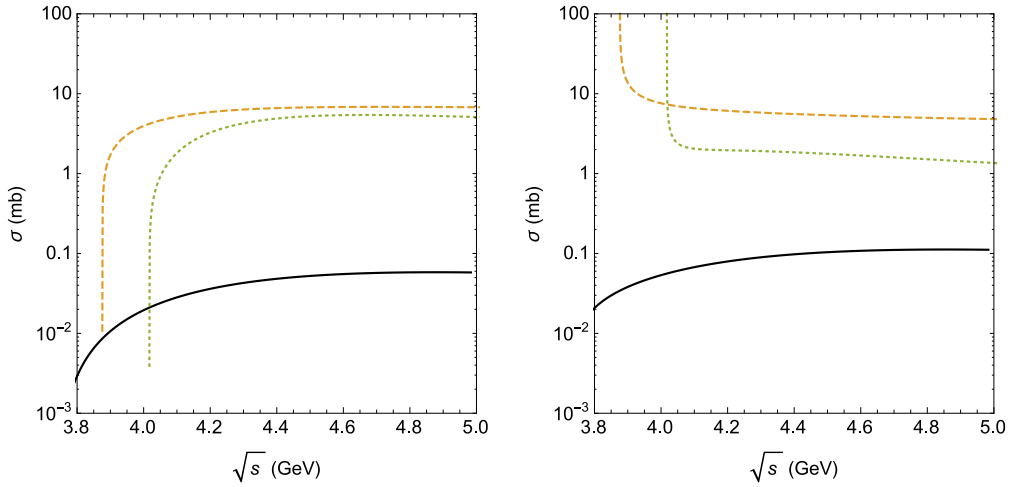

Figure 1. J/ψ absorption and production cross sections in different processes as a function of the CM energy $\sqrt{s}$. Left panel: $\pi J/\psi$ in the initial state. Solid, dashed and dotted lines represent the $\pi J/\psi \to D\bar{D}$, $\pi J/\psi \to D^*\bar{D}$ and $\pi J/\psi \to D^*\bar{D}^*$ reactions, respectively. Right panel: $\pi J/\psi$ in the final state. Solid, dashed and dotted lines represent the $D\bar{D} \to \pi J/\psi$, $D^*\bar{D} \to \pi J/\psi$ and $D^*\bar{D}^* \to \pi J/\psi$ reactions, respectively.

From these curves we can see that, excluding the low energy region (which will be much less relevant for phenomenology), the J/ψ production and absorption cross sections are very close to each other in almost all channels. Since the J/Ψ absorption and production cross sections have comparable magnitudes, what will determine the final yield of J/Ψ's will be the thermally averaged cross sections, which, reflecting the physical aspects of the hadron gas, will select the range of energies which are more important.

3. The role of exotic charmonium

In 2003 a new class of charmonium was discovered, the so-called exotic charmonium states (for recent reviews on the subject see Refs. [13, 14]). They are multiquark states composed by two quarks and two antiquarks ($c\bar{c}q\bar{q}$). As new members of the family they have a direct impact on the quarkonium - light hadron cross section, as it is illustrated in Fig. 2, where we show a new way to destroy (and also to regenerate) a J/ψ. In principle, the existence of these resonances in the s-channel could drastically change the $J/\psi - \pi$ cross section. Recently [8] we have calculated this effect and it turned out to be significant only in the energy region close to the reaction thresholds, being negligible elsewhere. This can be attributed to the narrow width of the resonances. These effects are illustrated in Fig. 3. On the left panel we see the J/Ψ absorption cross section by π's. The solid line represents the cross section obtained without including the Z_c (3900) exchange in the s-channel. The dashed line shows the result with the exchange of Z_c (3900) in the s-channel included. The right panel shows the J/Ψ absorption cross section by ρ. The solid line shows the cross section obtained without including the Z_c

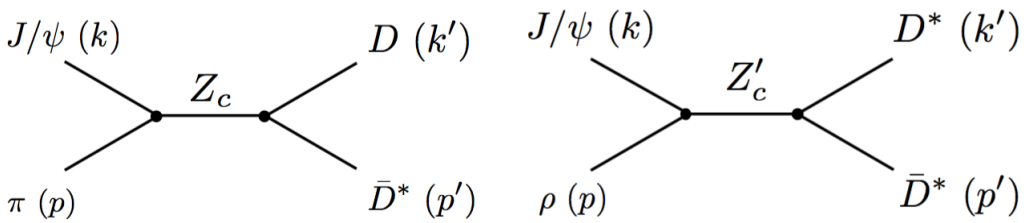

Figure 2. $J/\psi-\pi$ (left) and $J/\psi-\rho$ (right) reactions mediated by Z resonances in the s-channel.

(4025) exchange in the s-channel. The dashed line shows the result obtained by including the $Z_c(4025)$ exchange in the s-channel.

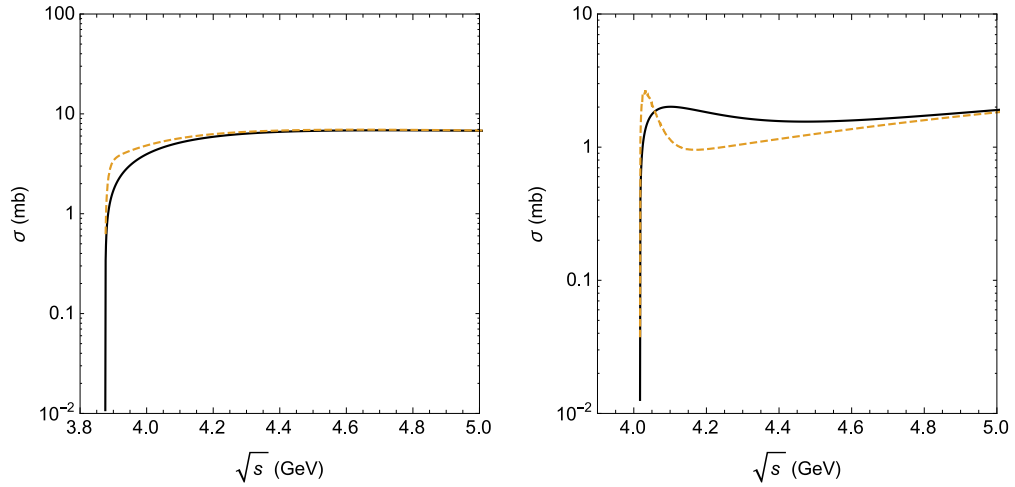

Figure 3. The left panel shows the J/Ψ absorption cross section by π's. The solid lines represent the cross sections obtained without including the Z_c (3900) exchange in the s-channel. The dashed lines show the results with the exchange of Z_c (3900) in the s-channel included. The right panel shows the J/Ψ absorption cross section by ρ. The solid line shows the cross sections obtained without including the Z_c (4025) exchange in the s-channel. The dashed line shows the results obtained by including the $Z_c(4025)$ exchange in the s-channel.

4. The effect of temperature

We define the thermally averaged cross section for a given process $ab \to cd$ as:

$$\langle \sigma_{ab\to cd}\, v_{ab} \rangle \;=\; \frac{\int d^3\mathbf{p}_a\, d^3\mathbf{p}_b\, f_a(\mathbf{p}_a)\, f_b(\mathbf{p}_b)\, \sigma_{ab\to cd}\; v_{ab}}{\int d^3\mathbf{p}_a\, d^3\mathbf{p}_b\, f_a(\mathbf{p}_a)\, f_b(\mathbf{p}_b)} \tag{10}$$

where v_{ab} represents the relative velocity of the two interacting initial particles a and b and the function $f_i(\mathbf{p}_i)$ is the Bose-Einstein distribution (of particles of species i), which depends on the temperature T.

In the two panels of Fig. 4 we plot the thermally averaged cross sections for $\pi J/\psi$ absorption (on the left) and production (on the right) via the processes discussed in previous section. We can see that for all processes the production reactions are larger than the absorption ones.

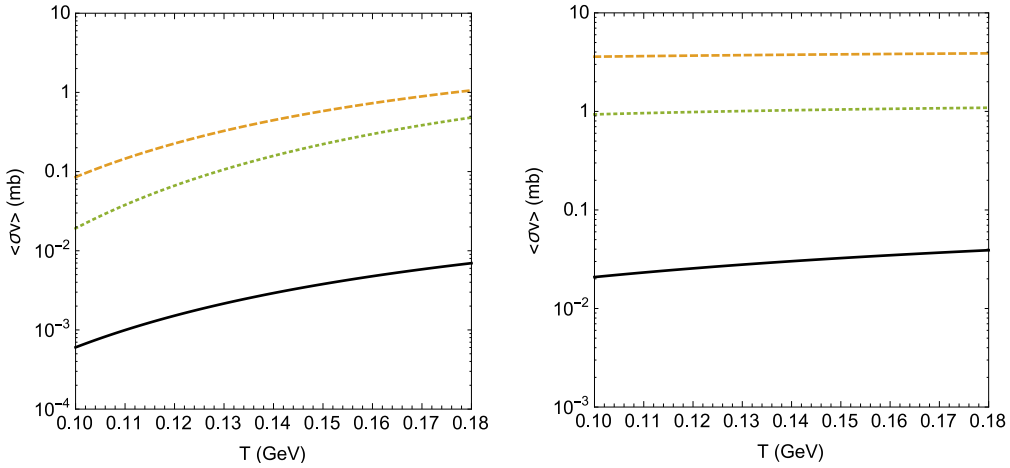

Figure 4. J/Ψ absorption and production cross sections by π's as a function of the temperature. Left panel: absorption reactions with $\pi J/\Psi$ in the initial state. $\pi J/\Psi \to D\bar{D}$ (solid line), $\pi J/\Psi \to D^*\bar{D}$ (dashed lines) and $\pi J/\Psi \to D^*\bar{D}^*$ (dotted lines). Right panel: production reactions with $\pi J/\Psi$ in the final state. The line convention is the same as in the left panel.

5. Time evolution of the J/ψ abundance

We complete this study by addressing the time evolution of the J/ψ abundance in hadronic matter, using the thermally averaged cross sections estimated in the previous section. We make use of the evolution equation for the abundances of particles included in processes discussed above. The momentum-integrated evolution equation has the form [15, 16, 17, 18]:

$$\begin{aligned}
\frac{dN_{J/\psi}(\tau)}{d\tau} = & \sum_{\varphi=\pi,\rho K,K^*} \Big[\langle\sigma_{D_{(s)}\bar{D}\to\varphi J/\psi} v_{D_{(s)}\bar{D}}\rangle n_{D_{(s)}}(\tau) N_{\bar{D}}(\tau) - \langle\sigma_{\varphi J/\psi\to D_{(s)}\bar{D}} v_{\varphi J/\psi}\rangle n_{\varphi}(\tau) N_{J/\psi}(\tau) \\
& + \langle\sigma_{D^*_{(s)}\bar{D}^*\to\varphi J/\psi} v_{D^*_{(s)}\bar{D}^*}\rangle n_{D^*_{(s)}}(\tau) N_{\bar{D}^*}(\tau) - \langle\sigma_{\varphi J/\psi\to D^*_{(s)}\bar{D}^*} v_{\varphi J/\psi}\rangle n_{\varphi}(\tau) N_{J/\psi}(\tau) \\
& + \langle\sigma_{D^*_{(s)}\bar{D}\to\varphi J/\psi} v_{D^*_{(s)}\bar{D}}\rangle n_{D^*_{(s)}}(\tau) N_{\bar{D}}(\tau) - \langle\sigma_{\varphi J/\psi\to D^*_{(s)}\bar{D}} v_{\varphi J/\psi}\rangle n_{\varphi}(\tau) N_{J/\psi}(\tau) \\
& + \langle\sigma_{D_{(s)}\bar{D}^*\to\varphi J/\psi} v_{D_{(s)}\bar{D}^*}\rangle n_{D_{(s)}}(\tau) N_{\bar{D}^*}(\tau) - \langle\sigma_{\varphi J/\psi\to D_{(s)}\bar{D}^*} v_{\varphi J/\psi}\rangle n_{\varphi}(\tau) N_{J/\psi}(\tau)\Big] \\
& + \sum_{\varphi=\bar{\pi},\bar{\rho},\bar{K},\bar{K}^*} \Big[\langle\sigma_{\bar{D}_{(s)}D\to\varphi J/\psi} v_{\bar{D}_{(s)}D}\rangle n_{\bar{D}_{(s)}}(\tau) N_{D}(\tau) - \langle\sigma_{\varphi J/\psi\to\bar{D}_{(s)}D} v_{\varphi J/\psi}\rangle n_{\varphi}(\tau) N_{J/\psi}(\tau) \\
& + \langle\sigma_{\bar{D}^*_{(s)}D^*\to\varphi J/\psi} v_{\bar{D}^*_{(s)}D^*}\rangle n_{\bar{D}^*_{(s)}}(\tau) N_{D^*}(\tau) - \langle\sigma_{\varphi J/\psi\to\bar{D}^*_{(s)}D^*} v_{\varphi J/\psi}\rangle n_{\varphi}(\tau) N_{J/\psi}(\tau) \\
& + \langle\sigma_{\bar{D}^*_{(s)}D\to\varphi J/\psi} v_{\bar{D}^*_{(s)}D}\rangle n_{\bar{D}^*_{(s)}}(\tau) N_{D}(\tau) - \langle\sigma_{\varphi J/\psi\to\bar{D}^*_{(s)}D} v_{\varphi J/\psi}\rangle n_{\varphi}(\tau) N_{J/\psi}(\tau) \\
& + \langle\sigma_{\bar{D}_{(s)}D^*\to\varphi J/\psi} v_{\bar{D}_{(s)}D^*}\rangle n_{\bar{D}_{(s)}}(\tau) N_{D^*}(\tau) - \langle\sigma_{\varphi J/\psi\to\bar{D}_{(s)}D^*} v_{\varphi J/\psi}\rangle\Big] ,
\end{aligned} \tag{11}$$

where $n_\varphi(\tau)$ are $N_\varphi(\tau)$ denote the density and the abundances of π, ρ, K, K^*, charmed mesons and their antiparticles in hadronic matter at proper time τ. From Eq. (11) we observe that

the J/ψ abundance at a proper time τ depends on the $\varphi J/\psi$ dissociation rate as well as on the $\varphi J/\psi$ production rate. We remark that in the rate equation we have also considered the processes involving the respective antiparticles, i.e. $\bar{\varphi} J/\psi \to \bar{D}_{(s)}^{(*)} D^{(*)}$ and $\bar{D}_{(s)}^{(*)} D^{(*)} \to \bar{\varphi} J/\psi$. We assume that π, ρ, K, K^*, D and D^* are in equilibrium. Therefore the density $n_i(\tau)$ can be written as [15, 16, 17, 18]

$$n_i(\tau) \approx \frac{1}{2\pi^2} \gamma_i g_i m_i^2 T(\tau) K_2 \left(\frac{m_i}{T(\tau)} \right), \tag{12}$$

where γ_i and g_i are respectively the fugacity factor and the degeneracy factor of the relevant particle. The abundance $N_i(\tau)$ is obtained by multiplying the density $n_i(\tau)$ by the volume $V(\tau)$. The time dependence is introduced through the temperature $T(\tau)$ and volume $V(\tau)$ profiles appropriate to model the dynamics of relativistic heavy ion collisions after the end of the quark-gluon plasma phase. The hydrodynamical expansion and cooling of the hadron gas is modeled as in Refs. [15, 16, 17, 18] by a boost invariant Bjorken flow with an accelerated transverse expansion:

$$\begin{aligned} T(\tau) &= T_C - (T_H - T_F) \left(\frac{\tau - \tau_H}{\tau_F - \tau_H} \right)^{\frac{4}{5}}, \\ V(\tau) &= \pi \left[R_C + v_C (\tau - \tau_C) + \frac{a_C}{2} (\tau - \tau_C)^2 \right]^2 \tau_C. \end{aligned} \tag{13}$$

In the equation above, R_C and τ_C fm/c denote the final transverse and longitudinal sizes of the quark-gluon plasma, while v_C and a_C are its transverse flow velocity and transverse acceleration at this time. $T_C = 175$ MeV is the critical temperature for the quark-gluon plasma to hadronic matter transition; $T_H = T_C = 175$ MeV is the temperature of the hadronic matter at the end of the mixed phase, occurring at the time τ_H. The freeze-out temperature $T_F = 125$ MeV then leads to a freeze-out time τ_F. In addition, we assume that the total number of charmed quarks in charmed hadrons is conserved during the processes. This number can be calculated with perturbative QCD and yields the charm quark fugacity factor γ_C in Eq. (12) [15, 16, 17, 18]. The total number of pions and ρ mesons at freeze-out was taken from Refs. [19, 20]. In the case of $K^{(*)}$ and $\bar{K}^{(*)}$ mesons [15], we work with the assumption that strangeness reaches approximate chemical equilibrium in heavy ion collisions due to the short equilibration time in the quark-gluon plasma and the net strangeness of the QGP is zero.

We will study the J/ψ evolution in the hadron gas formed in two types of collisions: central $Au - Au$ collisions at $\sqrt{s_{NN}} = 200$ GeV at RHIC and central $Pb - Pb$ collisions at $\sqrt{s_{NN}} = 5$ TeV at the LHC. The parameters which we need as input in Eqs. (13) are listed in Table 3.1 of Ref. [15] and, for convenience, are reproduced in Table 1.

Table 1. Parameters used in the parametrization of the hydrodynamical expansion, given by Eqs.(13).

	v_C (c)	a_C (c^2/fm)	R_C (fm)	τ_C (fm/c)	τ_H (fm/c)	τ_F (fm/c)	γ_c	$N_{J/\psi}$
RHIC	0.4	0.02	8	5	7.5	17.3	6.4	0.017
LHC	0.6	0.044	13.11	5	7.5	20.7	15.8	1.67

In Fig. 5 we present the time evolution of the J/ψ abundance as a function of the proper time for the two types of collisions discussed above: at RHIC (on the left panel) and at the LHC (on the right panel). Looking at the evolution equation, Eq. (11), we can see that the fate of the J/ψ population will be determined by the production and absorption cross sections

and by the multiplicities of the other mesons, especially the pion multiplicity. While the cross sections alone would favor an enhancement of the J/ψ yield, the relative multiplicities favor its reduction, since in the hadron gas there are much more pions and kaons (which hit and destroy the charmonium states) than D's, $\bar{D}$'s, D_s's and $\bar{D}_s$'s (which can collide and create them). The result of this competition is a decrease of the J/ψ yield of approximately 20 % at RHIC and 24 % at the LHC. From the solid line in the figure we can see that if there were only pions in the gas, there would be a small suppression of the J/ψ yield. This comes from a cancellation between a difference in the cross sections favoring production with a large difference in multiplicities, as pions are much more abundant than open charm mesons. The same competition occurs if the gas would include ρ's, kaons and K^*'s.

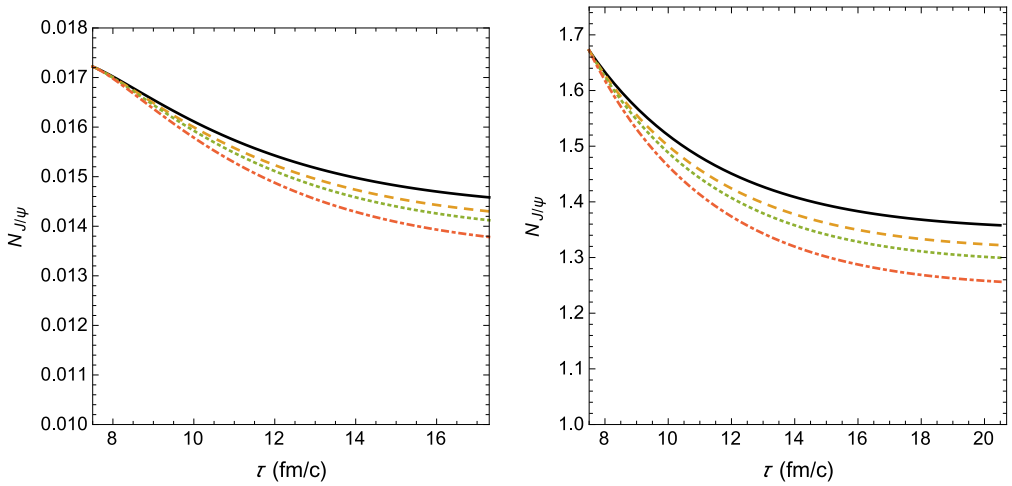

Figure 5. Left: Time evolution of J/ψ abundance as a function of the proper time in central Au-Au collisions at $\sqrt{s_{NN}} = 200$ GeV. Solid, dashed, dotted, dot-dashed lines represent the situations with only $\pi - J/\psi$ interactions and also adding the $\rho - J/\psi$, $K - J/\psi$ and $K^* - J/\psi$ contributions, respectively. Right: the same as on the left for LHC conditions.

6. Time evolution of the Υ abundance

While charmonium states have been extensively studied as QGP probes, bottomonium states were not explored so much, even though the $b\bar{b}$ family of states provides experimentally more robust and theoretically cleaner probes. Moreover, bottomonium states are regarded as better probes because recombination effects are believed to be much less significant than in the charmonium case. Although the recombination effect is expected to increase for bottomonia from RHIC to LHC energies, it is predicted to remain small [21, 22, 23, 24, 25, 26, 27].

From the experimental side, the CMS detector has excellent capabilities for muon detection and provides measurements of the Υ family which enable the accurate analysis of bottomonium [28] production. For this reason, the main interest may be shifted to the suppression of bottomonium states at LHC energies. The first indication of Υ suppression in heavy ion collisions was reported by CMS in 2011 [29]. Later it was also observed by the STAR Collaboration at RHIC [30]. The $\Upsilon(2S)$ and $\Upsilon(3S)$ resonances in PbPb collisions were seen to be more strongly suppressed than the $\Upsilon(1S)$ (compared with the pp result), showing the expected sequential suppression pattern [28].

The most recent data on prompt J/ψ [31] and Υ [28, 32, 33, 34] suppression in the most central Pb Pb collisions at small rapidities and small p_T, show that:

$$R_{AA}(J/\psi) \simeq 0.28 \pm 0.03 \tag{14}$$

and

$$R_{AA}(\Upsilon(1S)) \simeq 0.38 \pm 0.05 \tag{15}$$

These factors are very weakly dependent on the collision energy $\sqrt{s}_{NN}$. Although they are close to each other, they may be the result of a quite different dynamics.

After the QGP cooling and hadronization there is a hadron gas (HG) phase. Apart from being a reasonable assumption, the existence of this phase seems to be necessary to correctly reproduce [35] the multiplicities of K^* and ρ measured by the ALICE Collaboration [36, 37, 38]. Heavy quarkonium is produced at the beginning of the heavy ion collision. Then it may be destroyed and regenerated both in the quark gluon plasma and in the subsequent hadron gas. The observed Υ suppression has been explained mostly with models which take into account only what happens during the QGP phase. In [39] we addressed the contribution of the hadron gas phase to the Υ production and absorption.

In the literature, there is a large number of works on quarkonium interactions with light mesons in a hot hadron gas using different approaches (for a short and recent compilation of references on charmonium interactions, see [40]). Many of these works investigate the J/ψ-light meson reactions based on effective hadron Lagrangians [40, 41, 6, 42]. After a long series of works, different groups found a similar value of the $J/\psi - \pi$ cross section, which is close to the value obtained with QCD sum rules [12]. In [40], we have used all the known charmonium-light hadron absorption cross sections (together with the inverse interactions in which charmonium is produced) as input to solve the rate equation which governs the time evolution of J/ψ abundance in a hadron gas.

In contrast to the J/ψ case, the number of studies about the Υ interactions with light hadrons is much smaller [43]. In fact, to the best of our knowledge, the paper by Lin and Ko, Ref. [7], is the only one to give an estimate of the cross sections for scattering of Υ by pions and ρ mesons in a hot hadron gas. In that work the authors used a hadronic Lagrangian based on the SU(5) flavor symmetry. Including form factors with a cutoff parameter of 1 or 2 GeV at the interaction vertices, they found that the values of $\sigma_{\pi\Upsilon}$ and $\sigma_{\rho\Upsilon}$ are about 8 mb and 1 mb, respectively. However their thermal averages at a temperature of 150 MeV are both around only 0.2 mb. The reason for this reduction comes from the momentum average made in the thermal average. The kinematical threshold plays an important role since the sum of the masses of the initial state is $\simeq$ 9597 MeV and the sum of the masses of the final $B\bar{B}$ state (the lightest one) is $\simeq$ 10558. Hence their difference is $\simeq$ 960 MeV, which is still much larger than the temperature, $\simeq$ 150 MeV, and it is responsible for the strong reduction from 8 mb to 0.2 mb. They then conclude speculating that the absorption of directly produced Υ by comoving hadrons is unlikely to be important. In [39] we contributed to this subject extending the analysis performed in Ref. [40] to the bottomonia sector: we investigated the interactions of Υ with the surrounding hadronic medium composed of the lightest pseudoscalar meson (π) and the lightest vector meson (ρ). We calculated the cross sections for processes such as $\bar{B}^{(*)} + B^{(*)} \to \Upsilon + (\pi, \rho)$ scattering and their inverses, within the effective hadron Lagrangian framework. We improved the previous calculation introducing anomalous interactions. The obtained cross sections were used as input to solve the rate equation which allows us to follow the time evolution of the Υ multiplicity.

The importance of the anomalous vertices has been earlier mentioned in different contexts. For example, in Ref. [6] the J/ψ absorption cross sections by pions and ρ mesons were evaluated for several processes producing D and D^* mesons in the final state. The authors found that the $J/\psi\pi \to D^*\bar{D}$ cross section obtained with the exchange of a D^* meson in the t-channel, which

involves the anomalous $D^*D^*\pi$ coupling, was around 80 times bigger than the one obtained with a D meson exchange in the t-channel.

As it was pointed out in [39], the introduction of anomalous interactions leads to a strong hadronic suppression of Υ instead of the weak suppression expected in [7]. If confirmed these results indicate that, in contrast to the J/ψ case, the Υ's are produced in the QGP, their number remains nearly constant throughout the plasma phase and their suppression takes place in the hadron gas phase.

The diagrams representing the Υ interactions are shown in Figs. 6 and 7. Repeating the

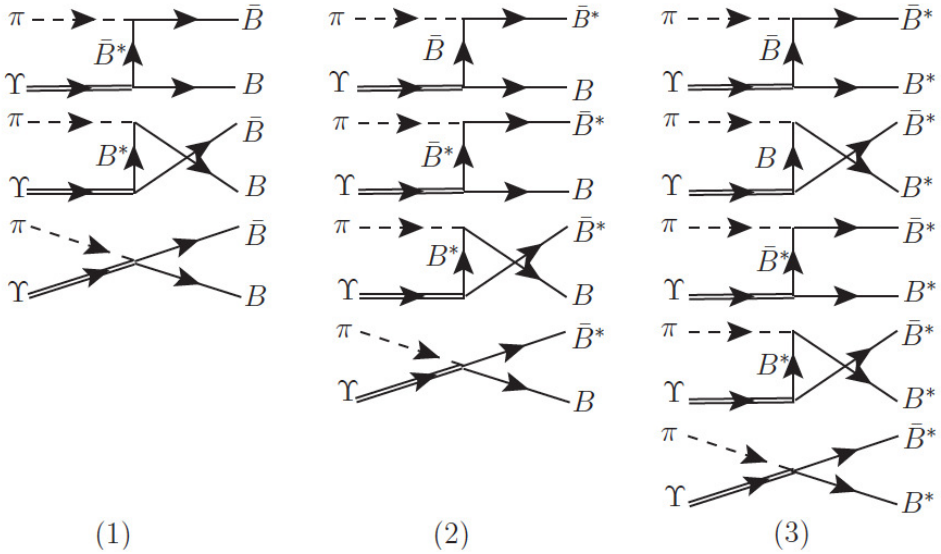

Figure 6. Diagrams contributing to the processes: (1) $\pi\Upsilon \to \bar{B}B$, (2) $\pi\Upsilon \to \bar{B}^*B$, and (3) $\pi\Upsilon \to \bar{B}^*B^*$.

steps described above for the case of the charmonium, we can compute the cross sections for absorption and production of Υ, their thermal averages and finally the evolution equation for the Υ abundance.

From Fig. 8 we can see that excluding the low energy region (which will be much less relevant for phenomenology), the Υ production and absorption cross sections are close to each other. Therefore, taking into account that the Υ absorption and production cross sections have comparable magnitudes, the computation of thermally averaged cross sections is an essential step to determine the final abundance of Υ's.

In Fig. 9 we plot the thermally averaged cross sections for $\pi\Upsilon$ absorption (left panel) and production (right panel) via the processes discussed above. As can be seen, in general, the production reactions have larger cross sections than the corresponding inverse reactions.

The range of temperatures which is relevant for our discussion corresponds to a very narrow range of energies $\sqrt{s}$, not far from the reaction reaction thresholds. The lines in Fig. 9 preserve the relative importance of the channels and they reproduce what is observed in Fig. 8. In other words, the thermal averaging does not change the relative ordering of the cross sections.

The time evolution of the Υ abundance is plotted in Fig. 10 as a function of the proper time, for the two types of collisions discussed above: at RHIC (on the upper panel) and at the LHC (on the lower panel).

The behavior of the Υ multiplicity observed in Fig. 10 is not difficult to understand. Due to the assumption that the hadronic stage at LHC is longer compared to that at RHIC, more

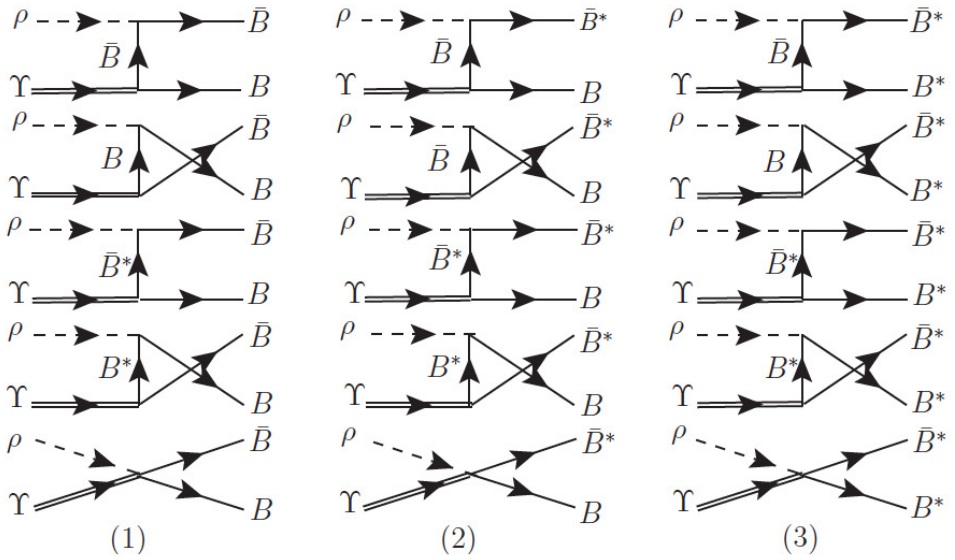

Figure 7. Diagrams contributing to the processes: (1) $\rho\Upsilon \to \bar{B}B$, (2) $\rho\Upsilon \to \bar{B}^*B$, and (3) $\rho\Upsilon \to \bar{B}^*B^*$.

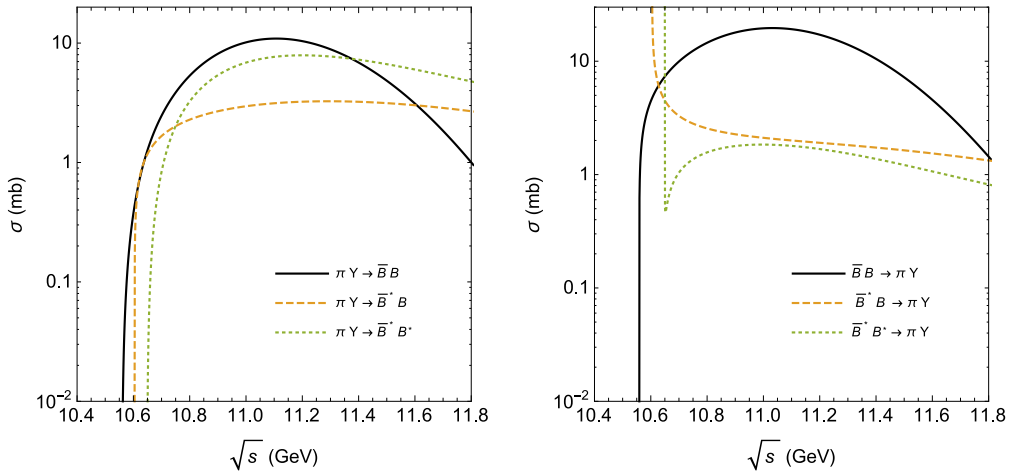

Figure 8. Υ absorption and production cross sections in different processes as a function of the CM energy $\sqrt{s}$. Left panel: $\pi\Upsilon$ in the initial state. Solid, dashed and dotted lines represent the $\pi\Upsilon \to \bar{B}B$, $\pi\Upsilon \to \bar{B}^*B$ and $\pi\Upsilon \to \bar{B}^*B^*$ reactions, respectively. Right panel: $\pi\Upsilon$ in the final state. Solid, dashed and dotted lines represent the $\bar{B}B \to \pi\Upsilon$, $\bar{B}^*B \to \pi\Upsilon$ and $\bar{B}^*B^* \to \pi\Upsilon$ reactions, respectively.

bottomonium states are lost in the hadronic medium at LHC. Also, it can be noticed, from Eq. (11), that the evolution of the Υ multiplicity depends on the production and absorption cross sections and also on the abundances of the other mesons. Although the production cross sections are greater than the absorption ones, which would enhance the Υ yield, the relative meson multiplicities lead to its reduction, since there are much more light mesons (especially pions) in the hadron gas to collide and destroy the bottomonium states than $B^{(*)}$'s and $\bar{B}^{(*)}$'s

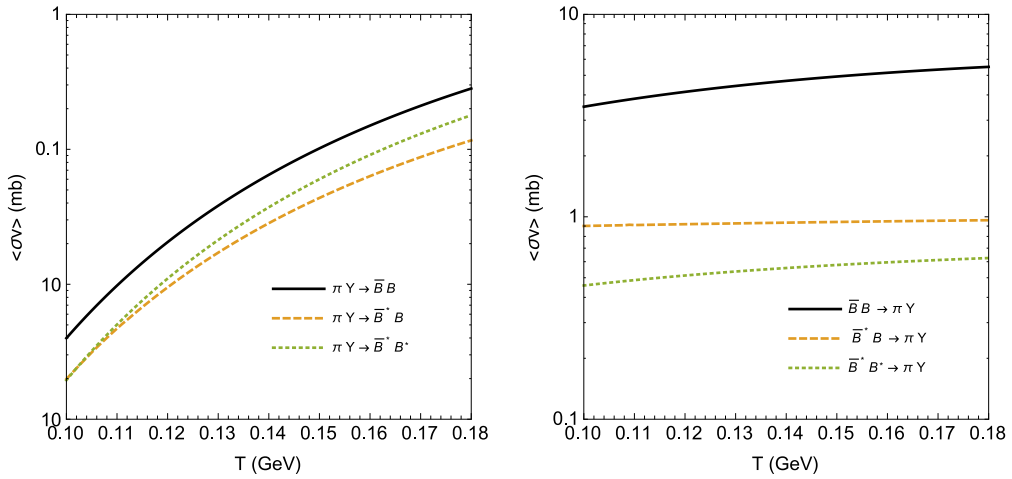

Figure 9. Thermally averaged cross sections for $\pi\Upsilon$ absorption and production as a function of the temperature. Left panel: $\pi\Upsilon$ in the initial state. Right panel: $\pi\Upsilon$ in the final state. Solid, dashed and dotted lines represent the reactions with $\bar{B}B$, $\bar{B}^*B$ and $\bar{B}^*B^*$, respectively, in final or initial state.

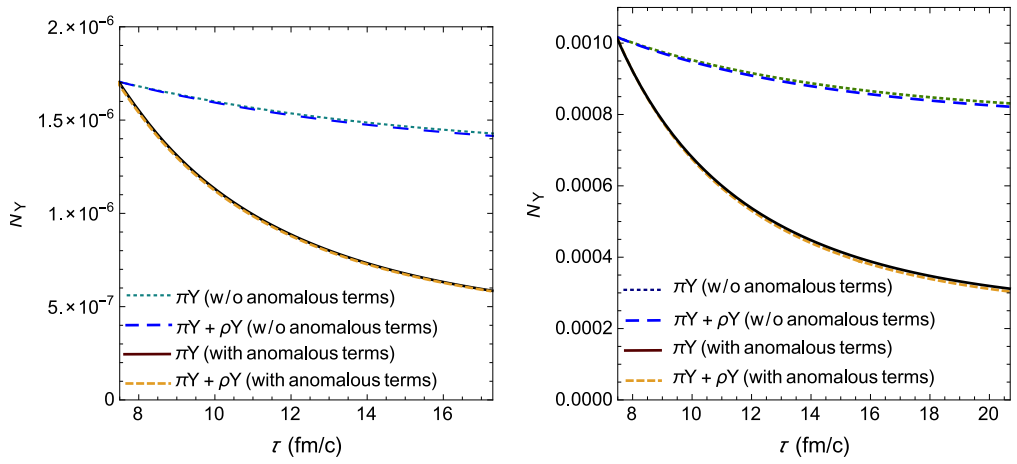

Figure 10. Left: Time evolution of Υ abundance as a function of the proper time in central Au-Au collisions at $\sqrt{s_{NN}} = 200$ GeV. Solid and dashed lines represent the situations with only $\pi - \Upsilon$ interactions and also adding the $\rho - \Upsilon$, respectively. Upper (lower) curves are calculated without (with) the anomalous interactions. Right: the same as on the left for LHC conditions.

to interact and create them. Besides, from the solid and dotted lines in Fig. 10 we can infer that the role of the ρ mesons in the gas is not relevant when compared to that of the pions. This comes from a cancellation between the terms associated to the production and absorption reactions: the different magnitudes of production and absorption processes are compensated by the relative multiplicities. Moreover we can see how important are the anomalous interactions. In both pannels, when we include them the upper curves move to the lower curves and the suppression increases by a factor $\simeq 3$.

The results shown in Fig. 10 suggest a decrease of the Υ yield of almost $\simeq 66$ % at RHIC and $\simeq 70$ % at the LHC. These numbers are compatible with (15). Taken literally, they would

suggest that all the suppression comes from the hadron gas phase. However we are not yet in the position of sustaining this strong statement. Before that, there is a number of points to be discussed. First the interactions in the reactions are naturally dependent on the effective formalism considered, which determines the magnitudes of the cross sections. A change in the magnitude of the production reactions will modify those of the absorption in the same proportion. This will lead to an overall multiplicative factor in the right hand side of rate equation, Eq. (11), modifying the curves in Fig. 10. Besides, our results are strongly dependent on the form factors and cutoff values: different choices would modify the slope of the curves in Fig. 10. Furthermore, the relevance of the parametrization of the hydrodynamical expansion exhibited in Eq. (13) can not be underestimated. Different parameters can make the system cool faster or slower and accordingly change the multiplicities of the distinct particles.

Notwithstanding the points raised above, we stress the main result: a reduction of the number of Υ's in the hadron gas, which seems to be larger than in the case of J/ψ reported in Ref. [40]. Before closing this section, we show in Fig. 11 a comparison between the Υ and J/ψ multiplicities as a function of the proper time. For the sake of comparison we have rescaled them to the unity at the initial time. The J/ψ suppression is only of $\simeq 25$ %, whereas it is of $\simeq 70$ % in the case of the Υ.

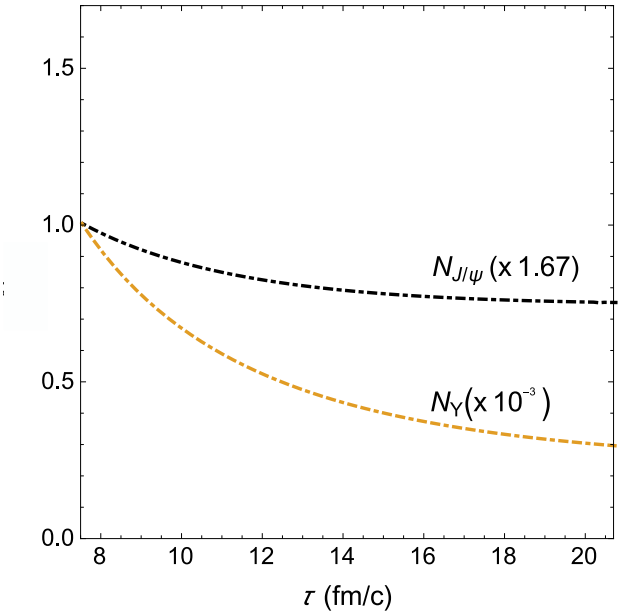

Figure 11. Time evolution of J/ψ (upper line) and Υ (lower line) abundances as a function of the proper time in central Pb-Pb collisions at the LHC.

7. Conclusions

Precise measurements of J/ψ abundancies in heavy ion collisions are an important source of information about the properties of the quark-gluon plasma phase. During this phase J/ψ is produced by recombination of charm-anticharm pairs. However, after hadronization the J/ψ's interact with other hadrons in the expanding hadronic matter. Therefore, the J/ψ's can be destroyed in collisions with other comoving mesons, but they can also be produced through the

inverse reactions. In order to evaluate the hadronic effects on the J/ψ abundance in heavy ion collisions one needs to know the J/ψ cross sections with other mesons.

We have studied J/ψ dissociation and production reactions, making use of effective field Lagrangians to obtain the cross sections for the processes $(\pi, \rho, K, K^*) + J/\psi \rightarrow D_{(s)}\bar{D}, D_{(s)}^{(*)}\bar{D}, D_{(s)}\bar{D}^{(*)}, D_{(s)}^{*}\bar{D}^{*}$ and the corresponding inverse processes. We have then computed the thermally averaged cross sections for the dissociation and production reactions, the latter being larger. Finally, we have used the thermally averaged cross sections as input in a rate equation and have followed the evolution of the J/ψ abundance in a hadron gas.

With respect to the existing calculations, the improvements introduced in [8] are the inclusion of K and K^*'s in the effective Lagrangian approach (and the computation of the corresponding cross sections) and the inclusion of processes involving the new exotic charmonium states $Z_c(3900)$ and $Z_c(4025)$.

We conclude that the interactions between J/ψ and all the considered mesons reduce the original J/ψ abundance (determined at the end of the quark gluon plasma phase) by 20 % and 24 % in RHIC and LHC collisions respectively. Consequently, any really significant change in the J/ψ abundance comes from dissociation and regeneration processes in the QGP phase.

We have also discussed here the hadronic effects on the Υ abundance in heavy ion collisions. Effective Lagrangians have been used to calculate the cross sections for the Υ-production processes $\bar{B}^{(*)} + B^{(*)} \rightarrow \Upsilon + (\pi, \rho)$, and also for the corresponding inverse processes associated to the Υ absorption. We have also computed the thermally averaged cross sections for the dissociation and production reactions. Finally, we have employed the thermally averaged cross sections as inputs in the rate equation and have determined the time evolution of the Υ abundance in a hadron gas. In Ref. [39] we introduced the following improvements: inclusion of reactions which start or end with $\bar{B}B$ and $\bar{B}^*B^*$ in the case of the pion-Υ scattering, and $\bar{B}^*B$ in that involving ρ meson; inclusion of the anomalous parity interactions processes in the effective Lagrangian approach.

Our results suggest that the interactions between Υ and light mesons reduce the Υ abundance at the end of the quark gluon plasma phase by $\simeq 70$ %, which is more than in the case of the J/ψ reported in Ref. [40].

In conclusion, despite the fact that there are points to be improved to obtain a more realist description of the HIC phenomenology, we believe that our findings are important for the physics of both the quark gluon plasma and hadronic phases. Our result should encourage further studies of the Υ suppression in the hadron gas phase of relativistic heavy ion collisions.

8. Acknowledgments

This work was partially supported by FAPESP and CNPq.

9. References

[1] Adams J *et al.* 2005 *Nucl. Phys.* **A757** 102 ; Aarts G *et al.* 2017 *Eur. Phys. J.* **A53**, 93
[2] For a recent review, see Braun-Munzinger P, Koch V, Schafer T and J. Stachel 2016 *Phys. Rept.* **621** 76
[3] Matsui T and Satz H 1986 *Phys. Lett.* **B178** 416
[4] Thews R L, Schroedter M and Rafelski J 2001 *Phys. Rev.* **C63** 054905; Braun-Munzinger P and Stachel J 2000 *Phys. Lett.* **B490**, 196
[5] Matinyan S G and B. Müller B 1998 *Phys. Rev.* **C58** 2994
[6] Oh Y, Song T and Lee S H 2001 *Phys. Rev.* **C63** 034901
[7] Lin Z and Ko C M 2001 *Phys. Lett.* **B503** 104

[8] Abreu L M, Khemchandani K P, Martinez Torres A, Navarra F S and Nielsen M 2018 *Phys. Rev.* **C97** 044902
[9] Azevedo R S and Nielsen M 2004 *Phys. Rev.* **C69** 035201; Azevedo R S and Nielsen M 2004 *Braz. J. Phys.* **34** 272
[10] Azevedo R S and Nielsen M (*Preprint* nucl-th/0407080)
[11] Bracco M E, Chiapparini M, Navarra F S and Nielsen M 2012 *Prog. Part. Nucl. Phys.* **67** 1019; Osorio Rodrigues B, Bracco M E, Nielsen M and Navarra F S 2011 *Nucl. Phys.* **A852** 127; Bracco M E, Chiapparini M, Navarra F S and Nielsen M 2008 *Phys. Lett.* **B659** 559; Bracco M E, Chiapparini M, Navarra F S and Nielsen M 2005 *Phys. Lett.* **B605** 326; Navarra F S, Nielsen M and Bracco M E 2002 *Phys. Rev.* **D65** 037502 ; Navarra F S, Nielsen M, Bracco M E, Chiapparini M and Schat C L 2000 *Phys. Lett.* **B489** 319; Bracco M E, Chiapparini M, Lozea A, Navarra F S and M. Nielsen 2001 *Phys. Lett.* **B521** 1; Bracco M E, Navarra F S and M. Nielsen 1999 *Phys. Lett.* **B454** 346
[12] Duraes F O, Kim H c, Lee S H, Navarra F S and Nielsen M 2003 *Phys. Rev.* **C68** 035208; Duraes F O, Lee S H, Navarra F S and Nielsen M 2003 *Phys. Lett.* **B564** 97; Navarra F S, Nielsen M, Marques R S de Carvalho and Krein G 2002 *Phys. Lett.* **B529** 87
[13] For a review on charged exotic charmonium states, see Nielsen M and Navarra F S 2014 *Mod. Phys. Lett.* **A29** 1430005
[14] For a very recent review, see Albuquerque R M, Dias J M, Khemchandani K P, Martinez Torres A, Navarra F S, Nielsen M and Zanetti C (*Preprint* arXiv:1812.08207)
[15] Cho S *et al.* 2011 *Phys. Rev.* **C84** 064910
[16] Cho S *et al.* 2017 *Prog. Part. Nucl. Phys.* **95** 279
[17] Cho S *et al.* 2011 *Phys. Rev. Lett.* **106** 212001
[18] Cho S and Lee S H 2018 *Phys. Rev.* **C97** 034908
[19] Chen L W, Ko C M, Liu W and M. Nielsen 2007 *Phys. Rev.* **C76** 014906
[20] Cho S and Lee S H 2013 *Phys. Rev.* **C88** 054901
[21] Aarts G *et al.*, 2017 *Eur. Phys. J.* **A53** 93
[22] Du X, Rapp R and He M 2017 *Phys. Rev.* **C96** 054901
[23] Andronic A, Braun-Munzinger P, Redlich K and Stachel J 2007 *Phys. Lett.* **B652**, 259; Gorenstein M I, Kostyuk A P, Stoecker H and Greiner W 2001 *Phys. Lett.* **B509** 277
[24] Liu Y et al. 2011 *Phys. Lett.* **B697** 32; Zhou K, Xu N and Zhuang P 2014 *Nucl. Phys.* **A931** 654
[25] Emerick A, Zhao X and Rapp R 2012 *Eur. Phys. J.* **A48** 72
[26] Krouppa B and Strickland M 2016 *Universe* **2** 16
[27] Krouppa B, Ryblewski R and Strickland M 2015 *Phys. Rev.* **C92** 061901
[28] Hu Z, Leonardo N T, Liu T and Haytmyradov M 2017 *Int. J. Mod. Phys.* **A32** 1730015
[29] Chatrchyan S et al. 2011 *Phys. Rev. Lett.* **107** 052302; Hu Z 2011 *J. Phys.* **G38** 124071; Chatrchyan S et al. 2012 *J. High Energy Phys.* **05** 063
[30] Adamczyk L et al. 2014 *Phys. Lett.* **B735** 127; Erratum: 2015 *Phys. Lett.* **B743** 537
[31] Khachatryan V *et al.* 2017 *Eur. Phys. J.* **C77** 252
[32] A. M. Sirunyan et al. 2019 *Phys. Lett.* **B790** 270
[33] Khachatryan V et al. 2017 *Phys. Lett.* **B770** 357
[34] Khachatryan V et al. 2017 *Phys. Lett.* **B764** 031
[35] Shapoval V M, Braun-Munzinger P and Sinyukov Y M 2017 *Nucl. Phys.* **A968** 391
[36] Adam J et al. 2017 *Phys. Rev.* **C95** 064606
[37] Abelev B B et al. 2015 *Phys. Rev.* **C91** 024609
[38] Riabov V G et al. 2017 *J. Phys. Conf. Ser.* **798** 012054; Markert C et al. 2017 *J. Phys. Conf. Ser.* **878** 012003
[39] Abreu L M, Navarra F S and Nielsen M 2018 *Preprint* arXiv:1807.05081
[40] Abreu L M, Khemchandani K P, Martínez Torres A , Navarra F S and Nielsen M 2018 *Phys. Rev.* **C97** 044902
[41] Matinyan S G and Müller B 1998 *Phys. Rev.* **C58** 2994; Bourque A and Gale C 2009 *Phys. Rev.* **C80** 015204; Bourque A and Gale C 2008 *Phys. Rev.* **C78** 035206; Bourque A, Gale C and Haglin K L 2004 *Phys. Rev.* **C70** 055203; Lin Z and Ko C M 2000 *Phys. Rev.* **C62** 034903; Lin Z and Ko C M 2001 *J. Phys.* **G27** 617; Navarra F S, Nielsen M and Robilotta M R 2001 *Phys. Rev.* **C64** 021901; Haglin K L and Gale C 2001 *Phys. Rev.* **C63** 065201; Haglin K L 2000 *Phys. Rev.* **C61** 031902; Carvalho F, Duraes F O, Navarra F S and Nielsen M 2005 *Phys. Rev.* **C72** 024902
[42] Khemchandani K P, Martinez Torres A, Nielsen M and Navarra F S 2014 *Phys. Rev.* **D89** 014029
[43] Ferreiro E G and Lansberg J P 2018 *JHEP* **1810** 094